Journal of Molecular Catalysis A: Chemical 378 (2013) 263–272

Contents lists available at SciVerse ScienceDirect

Journal of Molecular Catalysis A: Chemical

journal homepage: www.elsevier.com/locate/molcata

Manganese porphyrin in solution and heterogenized in different materials mediates oxidation of hydrocarbons by iodosylbenzene

Gabriel Kaetan Baio Ferreira[a], Kelly Aparecida Dias de Freitas Castro[a], Guilherme Sippel Machado[a], Ronny Rocha Ribeiro[b], Katia Jorge Ciuffi[c], Gustavo Pimenta Ricci[c], Jacqueline Aparecida Marques[d], Shirley Nakagaki[a,*]

[a] Laboratório de Bioinorgânica e Catálise and Departamento de Química—Centro Politécnico, Universidade Federal do Paraná, Curitiba 81531990 (UFPR) PR, Brazil
[b] Laboratório de EPR da Região Sul, Departamento de Química—Centro Politécnico, Universidade Federal do Paraná (UFPR), Curitiba, PR, Brazil
[c] Unifran–Universidade de Franca, Franca, SP, Brazil
[d] Departamento de Química, UEPG, Ponta Grossa, PR, Brazil

ARTICLE INFO

Article history:
Received 20 February 2013
Received in revised form 28 June 2013
Accepted 29 June 2013
Available online 8 July 2013

Keywords:
Porphyrin
Heterogeneous catalysis
Oxidation
Silica
Self-assembly

ABSTRACT

We prepared a free base porphyrin (HP) containing hydroxy and methoxy groups in the mesophenyl substituents of the porphyrin ring. We then inserted Mn(III) ion into the resulting HP, to obtain MnP. We used silica synthesized by the sol–gel process to immobilize the MnP in either acidic or basic medium, which afforded the solids MnPA and MnPB, respectively. We also conducted the solvothermal Mn(III) ion insertion into HP, which furnished the self-structured solid MnPS. Because the MnP was catalytically active in homogeneous medium, we investigated the activity of all the prepared solids as heterogeneous catalysts in the oxidation of various hydrocarbons. MnPA, MnPB, and MnPS presented similar or higher activity than the homogeneous MnP in the oxidation of cyclooctene, cyclohexene, cyclohexane and *n*-heptane. Concerning alkane oxidation, the heterogeneous catalysts were more selective for the alcohol than the MnP in homogeneous solution. Moreover, the solid catalysts favored the oxidation of linear alkane, with selectivity toward the primary alcohol. We were able to recover all the solids at the end of the reaction and reuse them.

1. Introduction

Macrocyclic ligands such as porphyrins, phthalocyanines, and porphycenes can form complexes with a variety of transition metals in different oxidation states [1,2]. These ligands are often used as model compounds in studies involving biological systems, because they can mimic the catalytic activity of cytochrome P-450, catalase, and lignin peroxidase, among other enzymes [3]. The selectivity and efficiency of biological systems has motivated studies that employ model compounds—these models help investigate the mechanisms of oxidation and reduction reactions, aiming to obtain efficient size- and shape-selective catalytic centers [3–6].

From a structural viewpoint, synthetic metalloporphyrins (MPs) resemble the active center of heme-containing biological systems. Therefore, MPs are frequently investigated as model compounds and are applied in such areas as photodynamic therapy [7,8], chemical sensors [9], construction of supramolecular structures [10], cells and energy [11], and catalysts of various chemical reactions including oxidation processes [12].

MPs are catalytically active in both homogeneous (when the MP is soluble in the reaction medium) and heterogeneous systems (when the MP complex is not in the same phase as the substrate and the reaction solvent, due to its immobilization onto different solids or because it is structured as an insoluble material) [5,13–29].

In homogeneous systems, MPs usually undergo oxidative destruction of the porphyrin ring [2] which, together with other factors [3–6], contributes to low product yields. In contrast, in the biological system the protein matrix isolates the catalytic site, inhibiting oxidative destruction of the macrocyclic ligand and giving high product yields; another enzyme is necessary to catabolize the heme ligand [30].

In academic biomimetic studies, the oxidative destruction of MP can be reversed through the rational synthesis of more robust porphyrin ligands. Alternatively, the catalyst can be transferred from the reaction solution to a solid phase, making catalysis a heterogeneous process [1–6]. Catalyst heterogenization can be achieved by immobilizing the MP onto a rigid, inert support such as porous glass [31], cationic clays like montmorillonite [32], lamellar anionic synthetic compounds including layered double hydroxides

* Corresponding author. Tel.: +55 41 33613180; fax: +55 41 3361 3186.
E-mail addresses: shirleyn@ufpr.br, shirleynb17@gmail.com (S. Nakagaki).

1381-1169/$ – see front matter © 2013 Elsevier B.V. All rights reserved.
http://dx.doi.org/10.1016/j.molcata.2013.06.022

[13,33,34], and hydroxy salts [35], among other matrices [36–38].

More recently, a new strategy has been proposed for catalyst heterogenization: the soluble catalytic species is converted into an insoluble solid via a synthetic process that involves the formation of a supramolecular network. This process generates a microporous solid, the so-called metal-organic framework, or MOF [14,15,29,39–41].

Both of the abovementioned strategies have provided effective heterogeneous catalysts. These strategies have overcome two major drawbacks of homogeneous catalysis: (i) catalyst deactivation caused by oxidative destruction of the catalytic species and (ii) formation of inactive species via side reactions [2–4,6].

Porphyrins and other macrocyclic molecules are good building blocks for supramolecular structures: they have a rigid planar core measuring 1 nm^2. The peripheral positions of this core, especially the *meso* position of the macrocyclic ring, can easily bind to a large variety of chemical functions. Additionally, these macrocycles can coordinate metal ions of different oxidation states, providing a large number of algorithms to construct distinct supramolecular architectures, coordination polymers, and porous crystalline structures [14]. MOFs are the best-known class of materials originating from covalent interactions between these building blocks and metallic units (such as metal ions or clusters), culminating in mono (1D), bi (2D), or three-dimensional (3D) porous crystalline coordination polymers with high surface area and well-defined pores and channels [16,42]. The combination of these characteristics with the well-known features of MPs – inherent stability, unique optical properties, and synthetic versatility – enables MOFs to act as sensors, molecular separators, and catalysts of heterogeneous processes [15]. When these solids are used as heterogeneous catalysts, their structure, which consists of channels and pores, becomes important: the channels and pores confer the macrocycle catalytic efficiency as well as size- and shape-selectivity toward certain substrates [43–46].

Immobilization of catalytic species onto silica obtained by the hydrolytic sol–gel route is also an efficient tool to obtain highly pure, rigid, and inert catalytic solids The hydrolytic sol–gel process described by Stöber [47], which employs basic catalysis, often generates solid silica with spherical features [48], but this specific morphology has not been reported to change the catalytic results obtained with MPs immobilized onto silica [49,50]. Recently Ucoski et al. immobilized two neutral metalloporphyrins [Mn(TAPP)]Ac and [Fe(TAPP)]Cl (TAPP = 5,10,15,20-tetrakis(acetalphenyl porphyrin)) on silica obtained through the sol–gel process in acidic and basic conditions. Yields slightly lower or similar to those achieved in homogeneous medium were obtained for the MPs immobilized on silica. The two solid were easily recovered from the reaction medium and reused, and the recyclability capacity and retained activity upon reuse were demonstrated [50]. Farhadi et al. reported that Mn(III) (TDCPP)Cl, was covalently bound to a silica prepared by the sol–gel process and used as photocatalyst in a heterogeneous process for the selective and efficient oxidative decarboxylation of α-arylacetic acids with H_2O_2 at room temperature. The activity of the solid catalyst in the heterogeneous photocatalytic system was higher than that of a corresponding homogeneous one. The catalyst was reused several times without loss of its activity and selectivity [51]. Cai et al. prepared three types of hybrid materials based on silica-metalloporphyrins with Fe, Co and Mn porphyrin [APTCPP] (5-(4-allyloxy)phenyl-10,15,20-tri(4-chlorophenyl) porphyrin) also using the sol–gel process involving a thiol-ene polymerization reaction of the free base porphyrin with 3-mercaptopropyltrimethoxysilane. They investigated the solids as catalysts for the aerobic oxidation of cyclohexane. They found that the prepared hybrid materials were more efficient catalyst than the analogous non-supported metalloporphyrins for cyclohexane hydroxylation using O_2-ascorbate system and the metal ion in the porphyrins significantly affected the catalytic efficiencies of these hybrid materials [52].

A further advantage of heterogeneous catalysis is the possibility to recover and reuse the catalyst—the support-macrocyclic complex system is more stable than the macrocyclic complex in solution, making the catalytic process more profitable and allowing for future technological applications. Moreover, the solid catalyst is usually more efficient than its homogeneous counterpart: the catalyst-support interaction and the porous structure of the MOF solid give rise to unusual selectivity [53].

This paper uses a manganese(III) porphyrin (MnP) obtained from the ligand 5,10,15,20-tetrakis free base (4-hydroxy,3-methoxyphenyl) porphyrin (HP) as homogeneous and heterogeneous catalyst in oxidation reactions. We compare the catalytic activity of the target MnP in three different systems: in homogeneous medium, supported onto silica gel obtained by the sol–gel process, and arranged in an insoluble structured solid (Fig. 1).

2. Experimental

All the solvents and reagents were purchased from Aldrich, Merck, or Fluka and were used without purification, unless otherwise stated. *N*,*N*-Dimethylformamide (DMF) was distilled under reduced pressure and stocked over 4-Å molecular sieves. Pyrrole was distilled under reduced pressure prior to use. Alkenes (*cis*-cyclooctene and cyclohexene) were purified on an alumina column before use.

2.1. Synthesis

2.1.1. Free base porphyrin (HP), manganese porphyrin (MnP) and the self-structured material (MnPS)

The free base porphyrin (HP, [H_2(THMPP)]–[5,10,15,20-tetrakis (4-hydroxy, 3-methoxyphenyl)porphyrin]) was synthesized by the Adler–Longo's methodology [54,55]. Manganese(III) ion (manganese(II) acetate, metal ion/HP molar ratio = 10) was inserted into the purified HP under acetic acid reflux, for 6 h [56] giving the dark green complex named MnP ([Mn(THMPP)]–[5,10,15,20-tetrakis (4-hydroxy,3-methoxyphenyl)porphyrinato] manganese(III) acetate). HP and MnP were characterized by UV–vis and FTIR (Figs. S1 and S2a, supplementary material). Perpendicular microwave polarization X-band electron paramagnetic resonance (EPR) recorded for MnP showed no absorptions, as expected for the Mn(III) ion inserted into the porphyrin complex.

Vanillin was employed to synthesize the tetra substituted porphyrin because it is a cheap aldehyde in comparison to others containing hydroxyl groups aldehydes (almost four times cheaper than 4-hydroxybenzaldehyde). Our choice in a hydroxyphenyl porphyrin is based on the easiness of deprotonation of phenol groups both to form coordination polymers with metal centers and to covalently bind to silica during sol–gel process.

In a solvothermal reaction, HP and solid manganese(II) acetate (metal ion/HP molar ratio = 10) were reacted in DMF for 48 h, resulting in a black solid, MnPS. This material was characterized by reflectance UV–vis spectroscopy (which displayed bands relative to MnP), FTIR spectroscopy, EPR, powder X-ray diffraction (PXRD), and textural analysis by the BET method.

2.1.2. MnP immobilization onto silica—materials MnPA and MnPB

A MnP solution in methanol (22 mmol L^{-1}), tetraethyl orthosilicate (TEOS) (13 mmol), and deionized water (10 mL) were mixed in an Erlenmeyer flask, under magnetic stirring. Alcohol (ethanol for the acidic method or isopropyl alcohol for the

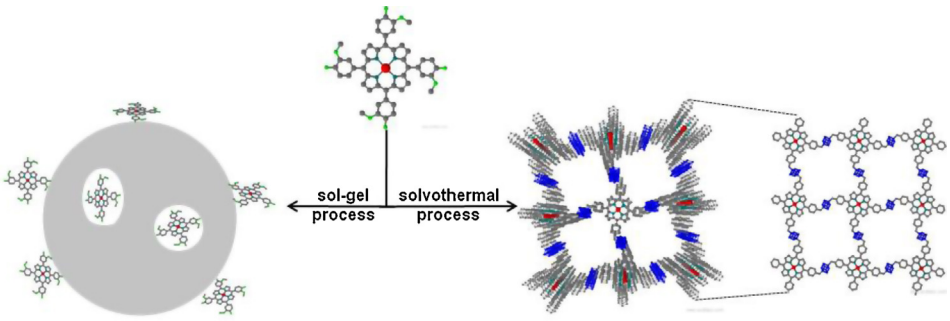

Fig. 1. Schematic representation of the manganese porphyrin (MnP, top, middle) and of the solids resulting from the heterogenization process: solid manganese porphyrin in silica prepared by the sol–gel process (MnPA and MnPB, bottom left, silica network represented by the grey circle with some metalloporphyrins encapsulated into its pores or adsorbed onto the surface); insoluble manganese porphyrin solid prepared by solvothermal process (MnPS, bottom right, tridimensional material and single sheet view).

basic method) (50 mmol) was then added to the flask, together with the hydrolysis-condensation catalyst (hydrochloric acid for the acidic or ammonium for the basic route) (2.5 mmol). The TEOS/alcohol/water molar ratio was kept at 1:4:40. The system was maintained under magnetic stirring for 30 min, at 60 °C, followed by aging for 25 days, at room temperature. The obtained glass solids, MnPA (obtained by acid catalysis) and MnPB (originated from basic catalysis), were exhaustively washed with methanol in a Sohxlet extractor for 24 h and dried under reduced pressure. The MnP loading on the silica (mol of MnP per gram of silica) was indirectly obtained: the amount of MnP removed from the silica during the washing procedures was determined by quantitative UV–vis analysis of the washing solutions; this amount was then subtracted from the initial quantity of MnP used in the immobilization procedure. MnPA and MnPB were characterized by UV–vis and FTIR spectroscopies, EPR, and textural analysis.

2.2. Catalytic activity tests

All the materials were tested as catalysts in the oxidation of different hydrocarbon substrates (*cis*-cyclooctene, cyclohexene, cyclohexane, and *n*-heptane), using iodosylbenzene (PhIO, prepared according to Saltzman and Sharefkin and periodically checked for purity by iodometric titration [57]) as oxidant and a catalyst/oxidant/substrate molar ratio of 1:10:1000. The reactions were carried out using dichloromethane/acetonitrile (DCM/ACN) 1:1 (v/v) as solvent mixture, for 1 h, at room temperature, under argon atmosphere. Products were quantified by gas chromatography using *n*-octanol as internal standard.

2.3. Characterization and apparatus

The UV–vis spectra were registered on a Varian Cary 100 Bio Spectrophotometer in the 200–800 nm range. The liquid samples were analyzed using a cell with 1-cm path length. A Teflon® support was employed for the solid samples.

The FTIR spectra were recorded on a Biorad 3500 GX spectrophotometer in the 400–4000 cm^{-1} range. The KBr pellets were obtained by crushing the solids (1 mg) with spectroscopic grade KBr (100 mg). All the spectra were collected with a resolution of 4 cm^{-1} and accumulation of 32 scans.

Room temperature and 77-K perpendicular microwave polarization X-band EPR was measured on a Bruker EMX microX spectrometer; 77-K parallel microwave polarization X-band EPR experiments were conducted on a Bruker Elexsys E500 spectrometer equipped with a Bruker ER4116DM dual mode resonator.

For the PXRD analysis, self-oriented films were placed on neutral glass sample holders. The patterns were obtained on a Shimadzu XRD-6000 diffractometer, in the reflection mode. The equipment was operated at 40 kV and 40 mA, using Cu K_α radiation (λ = 1.5418 Å) and a dwell time of 1 min^{-1}.

Textural analyses were carried out on the basis of the corresponding nitrogen (Air–liquid, 99.999%) adsorption at −196 °C, obtained from a static volumetric apparatus (Micromeritics ASAP 2020 adsorption analyzer). The samples (0.2 g) were degassed at 200 °C for 24 h (p < 0.133 Pa). The specific surface area was calculated by the BET method, and the total pore volume was estimated from the amount of nitrogen adsorbed at a relative pressure of 0.95.

All the products from the catalytic oxidation reactions were identified using an Agilent 6850 gas chromatograph (flame ionization detector) equipped with a DB-WAX capillary column with a length of 30 m and internal diameter of 0.25 mm (J&W Scientific). The oven temperature program used to determine the oxidation products from *cis*-cyclooctene, cyclohexene, and cyclohexane started at 100 °C. The temperature was then increased to 150 °C at 10 °C min^{-1}, followed by further temperature rise to 200 °C at 50 °C min^{-1}, which was maintained for 1 min. To determine the products originated from *n*-heptane, the temperature program started at 70 °C, followed by a temperature elevation to 100 °C at 5 °C min^{-1}, maintained for 1 min, and further temperature increase to 200 °C at 20 °C min^{-1}, kept for 1 min.

3. Results and discussion

3.1. HP, MnP, and MnPS

Condensation of pyrrole and vanillin via acid catalysis using Adler–Longo's methodology [54] furnished the free base porphyrin HP as a purple solid; its UV–vis spectrum displayed the typical Soret band at 426 nm (ε = 41,700 L mol^{-1} cm^{-1}), as well as the four Q-bands at 520, 558, 596, and 654 nm, characteristic of free base porphyrins (Fig. S1a, supplementary material).

The UV–vis spectrum of the green solid MnP presented a Soret band at 476 nm, due to the bathochromic shift undergone by manganese(III) porphyrins upon Mn(III) ion insertion into the free base porphyrin. The set of bands under 430 nm and the two Q-bands at 580 and 622 nm resulted from alteration in the microsymmetry of the porphyrin macrocycle from D_{2h} to D_{4h}, a consequence of the presence of the Mn(III) ion in the porphyrin core [55,58–61] (Fig. S1b, supplementary material).

The perpendicular microwave polarization X-band EPR of MnP did not evidence any absorption, as expected for manganese(III) porphyrins (data not shown) [62].

Mn(III) ion insertion into HP under solvothermal conditions gave a black insoluble solid (MnPS) with UV–vis spectral profile similar to the one achieved for the MnP obtained under conventional metal insertion conditions (solvent reflux). The reflectance UV–vis spectrum of MnPS revealed a Soret band at 426 nm,

attesting to the presence of the MnP in MnPS (Fig. S2, supplementary material).

The FTIR spectrum of MnPS (Fig. S3, supplementary material) presented the same pattern as the FTIR spectrum of MnP, confirming the presence of the MnP in the structure of MnPS. Bands relative to acetate as a counterion also appeared, as observed for MnP (difference between asymmetric and symmetric stretches equal to 172 cm^{-1} for MnP and 172 cm^{-1} for MnPS) [63,64] as expected for a manganese(III) porphyrin. The band at 1653 cm^{-1} may refer to C=O stretching from DMF molecules present in MnPS [65], adsorbed onto the walls of the material and/or coordinated to central metal site of manganese porphyrins [66,67].

The perpendicular microwave polarization X-band EPR spectra of MnPS at room temperature and 77 K were similar: there was intense absorption around $g = 2$, characteristic of species containing Mn(II) centers (Fig. 2a). In contrast, the EPR spectra of MnP, in the traditional EPR analysis (perpendicular polarization CW-EPR) shows no signal, as expected, due to the presence of only Mn(III) central species that are "silent" to this technique in the perpendicular mode. When MnPS is analyzed by parallel EPR (electron paramagnetic resonance, in which an oscillating magnetic field is applied parallel to the static magnetic field—parallel polarization CW-EPR[68]), transitions both for Mn(II) and Mn(III) are observed and these data suggested that manganese(III) species are also present in MnS solid. The EPR technique of parallel polarization is an useful tool for observing EPR spectra from integer electron spin systems such as found in many transition metals (Mn(III)). On the other hand conventional perpendicular mode EPR allows observation of half integer spin systems (Mn(IV), Mn(II), etc.) These signals suggest that MnPS, displaying Mn(III) in the core of the macrocycle (Fig. 2b) (a situation that does not generate any signal in perpendicular microwave polarization EPR), also contains Mn(II) species binding the macrocycles together in a supramolecular arrangement that resembles MOFs [41,62,68,69].

The PXRD analysis (Fig. 3) of the synthesized compounds revealed distinct patterns. The diffractograms of the starting salt $Mn(OAc)_2$ and of HP (Fig. 3a and b, respectively) agreed with the patterns reported in the literature [70]. MnP displayed a peak at $2\theta = 8.58^\circ$ (Fig. 3c), attributed to organization of the planar MnP after its insertion into the support used for the PXRD analysis–these planes can diffract the X-ray radiation, generating the diffraction peak. However, this diffraction did not directly relate to a structure with effective diffraction planes, as evidenced by the absence of secondary diffraction peaks in the analysis.

The PXRD pattern of MnPS (Fig. 3d) was different: compared with the diffractogram of MnP, the first peak shifted to $2\theta = 8.76^\circ$, corresponding to a distance of 10.08 Å. We ascribed this signal as the (0 0 1) peak [71]. We also detected the peaks (0 0 2), (0 0 3), and (0 0 5) [70], which show that MnPS presents more diffraction planes and is a more crystalline material than MnP. MnPS also displayed short-distance peaks in the 2θ range from 32° to 39°, relative to distances around 2.50 Å; these peaks probably refer to the distance between two metal ions in the structure and suggest that the crystalline structure of MnPS is different from the starting structure of MnP.

To evaluate the robustness of the synthesized MnPS crystalline network, we exhaustively dried MnPS under vacuum at room temperature [39], to eliminate traces of the solvent DMF, and analyzed the resulting solid by PXRD (Fig. 3e). Compared with the diffractogram in Fig. 3d, the diffractogram in Fig. 3e did not evidence any significant modifications. Thus, the structure of MnPS was not destroyed during the drying process, and its long-range order was preserved [72,73]. Next, we suspended MnPS in DMF for 6 h, for resolvation, and recorded a new PXRD diffractogram while MnPS was still wet (Fig. 3f). Again, we obtained a PXRD pattern similar to those depicted in Fig. 3d and e, except for the appearance of an amorphous halo, attributed to the action of DMF on MnPS. Therefore, the robust crystalline MnPS maintained its structure after cycles of drying and resolvation with DMF [14].

Table 1
Textural properties of the silica-based solids.

	MnPA	MnPB	SiA	SiB
MnP Loading (mol g^{-1})	5.11×10^{-6}	3.05×10^{-5}		
% MnP Immobilization	47	98		
S_{BET} ($m^2\ g^{-1}$)	383	317	368	315
Pore volume ($cm^3\ g^{-1}$)	0.29	0.84	0.28	0.74
Pore size (Å)	30.14	105.9	29.8	100.4

3.2. Materials based on silica—MnPA and MnPB

We obtained the MnP loadings in the materials MnPA and MnPB (mol of MnP per gram of silica) indirectly: first, we determined the amount of MnP removed from the silica during the washings of MnPA and MnPB by quantitative UV–vis analysis of the methanol washing solutions; we then subtracted this amount from the initial quantity of MnP used in the immobilization procedure, which furnished the following loadings MnPA**:** 5.11×10^{-6} mol of MnP g^{-1} of silica and MnPB: 3.05×10^{-5} mol g^{-1} of silica. We ground MnPA and MnPB and analyzed the powders by UV–vis diffuse reflectance spectroscopy. MnPA and MnPB displayed the same spectral profile as MnP, confirming the presence of the MnP in the silica network; no MnP demetallation occurred during the immobilization procedure, irrespective of the medium (acidic or basic) (figure not shown).

We obtained sixfold higher MnP loading in basic medium. The use of acid or basic catalyst during the hydrolytic sol–gel route accounted for the different MnP loadings in MnPA and MnPB. In basic medium, the hydroxyl groups at the phenyl rings of the MnP are probably deprotonated (vanillin residue has $pK_a = 7.78$), facilitating participation of the MnP in the hydrolysis and condensation reactions leading to the silica network.

We did not detect any signals around $g = 2$ in the perpendicular microwave polarization X-band EPR analysis of MnPA and MnPB at room temperature. Hence, MnPA and MnPB contain stable Mn(III) species [62,74].

The FTIR spectra of MnPA and MnPB and of the control solids SiA and SiB (silica generated via the same routes but in the absence of the MnP) were very similar (not shown)—only bands relative to silica deformation and stretching appeared; the MnP did not contribute to the spectra. MnPA and MnPB contained low concentrations of the MnP (less than 0.4% in mass); therefore, we were only able to visualize the intense Si–O bands. FTIR data: cm^{-1} (attribution)—956 (Si–OH), 1080 (Si–O–Si), 3465 (Si–OH) [63].

Interestingly, incorporation of the MnP during formation of the silica gel network did not change the textural properties of the silica (compare MnPA with SiA and MnPB with SiB in Table 1), which contrasts with results of other works [50]. The surface area of MnPA and MnPB was around 350 $m^2\ g^{-1}$. We had expected a larger surface area for the material obtained by basic catalysis, MnPB, rather than for the material synthesized by acid catalysis, MnPA [49,50]. However, MnPA required shorter gelation time, which culminated in a less ordered silica network. Compared with MnPB, the random arrangement of the silicate units in MnPA resulted in a larger surface area.

According to Table 1, basic catalysis afforded more porous materials with larger pore size. Basic catalysis generally furnishes highly branched structures; i.e., spherical particles, and large intercluster pores remain after solvent removal, due to steric effects.

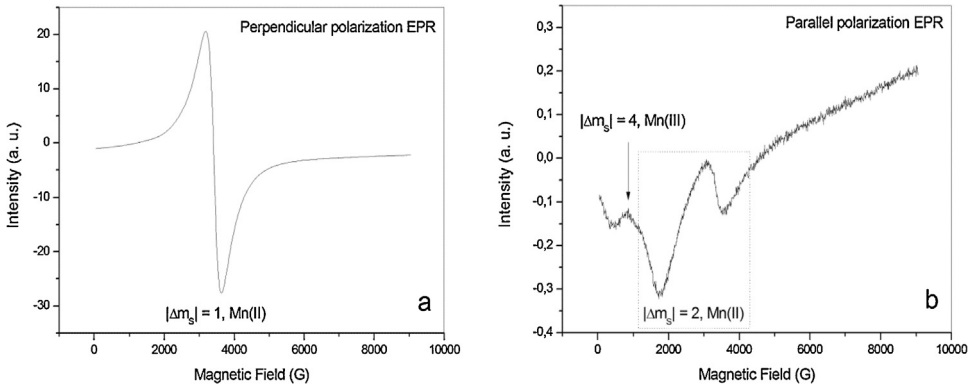

Fig. 2. 77-K X-band EPR MnPS spectra. (a) Perpendicular polarization. The intense absorption around 3500 G, characteristic of Mn(II) species, is due to a $\Delta m_S = \pm 1$ selection rule transition. (b) Parallel polarization. The $\Delta m_S = \pm 4$ transition, present as an absorption around 900 G, is due to Mn(III) species. The Mn(II) species also produce $\Delta m_S = \pm 2$ absorptions in the parallel polarization EPR experiment (B, dashed rectangle).

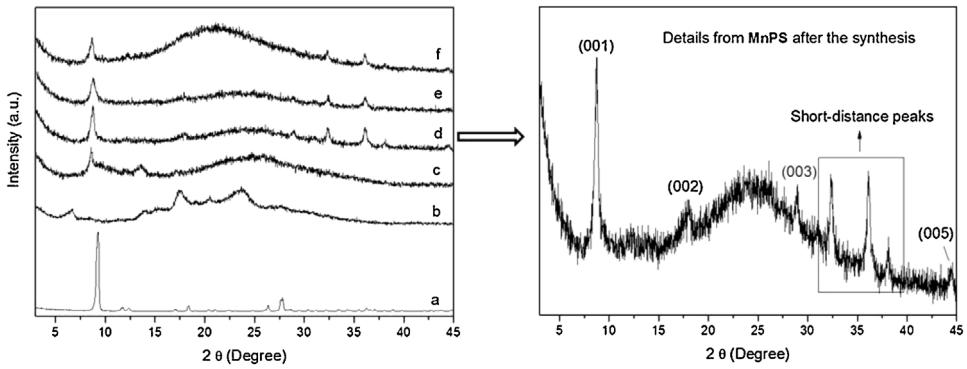

Fig. 3. Powder X-ray diffraction patterns of (a) $Mn(OAc)_2$, (b) HP, (c) MnP, (d) MnPS after synthesis, (e) MnPS after de-solvation under vacuum, and (f) MnPS after re-solvation with DMF.

Consequently, spheres with high degree of monodispersity are expected in this case. On the other hand, acid catalysis yields weakly branched systems and denser materials [75], but it does not favor monodispersity; the material is irregular, which justifies the larger surface area and the smaller pore size and volume of MnPA [76–78].

According to the IUPAC classification, the nitrogen adsorption/desorption isotherms of MnPA and MnPB (Fig. S4 and S5, supplementary material) are Type-IV [79]. Nevertheless, MnPA and MnPB have hysteresis H2 and H1, respectively. H2 hysteresis is characteristic of disordered/interconnected pores, but it can also indicate ink-bottle pores; H1 hysteresis relates to ordered and cylindrical pores open at both ends [79,80]. Again, the shorter gelation time required by MnPA when compared with MnPB explains these results.

3.3. Catalytic activity of the synthesized materials

We tested all the synthesized solids containing MnP in their structures (MnPS, MnPA, and MnPB) as heterogeneous catalysts in the oxidation of hydrocarbons; we used MnP in homogeneous medium for comparison (it is noteworthy that MnP was not totally soluble in the solvent mixture ACN:DCM). We also conducted control reactions without catalyst (homogeneous control reaction) or using pure silica gel prepared by the sol–gel process without immobilized MnP (heterogeneous control reaction). We investigated processes involving single oxygen transfer only—we used iodosylbenzene (PhIO, insoluble in the reaction medium) as the oxidant, and the model compounds acted as monooxygenases. We evaluated cyclic alkenes (*cis*-cyclooctene and cyclohexene) and alkanes (cyclohexane and heptane) as substrates (Fig. 4).

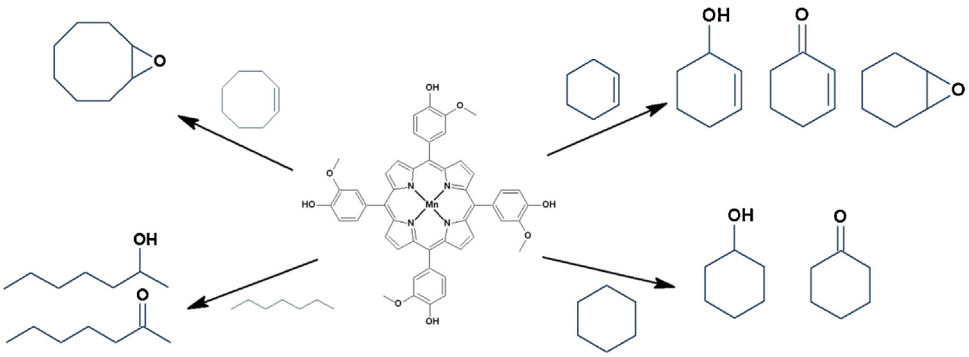

Fig. 4. Schematic representation of the oxidation of hydrocarbons catalyzed by the MnP studied herein (clockwise): *cis*-cyclooctene, cyclohexene, cyclohexane, and *n*-heptane.

Table 2
Yields of *cis*-cyclooctene epoxide from *cis*-cyclooctene oxidation by PhIO catalyzed by MnP systems[a].

Catalyst	Cyclooctene yield (%)[b]
MnP	54
MnPS	60
MnPS reuse	55
MnPA	35
MnPA reuse	31
MnPB	27
MnPB reuse	23
PhIO[c]	4.5
Silica + PhIO[d]	4.6
$Mn(OAc)_2$[e]	17

[a] Reactions carried out in duplicate. Reaction conditions: argon atmosphere, absence of light, magnetic stirring, room temperature, 60 min, DCM/ACN 1:1 (v/v) solvent mixture.
[b] Yields based on PhIO.
[c] Homogeneous control reaction.
[d] Heterogeneous control reaction.
[e] Control reaction using manganese(II) acetate tetrahydrate as catalyst in the same reaction conditions.

3.3.1. Oxidation of cis-cyclooctene

First, we used *cis*-cyclooctene as diagnostic substrate. Contrary to cyclohexene, which gives epoxide, alcohol, and/or ketone as products, *cis*-cyclooctene oxide is the only product generated during metalloporphyrin-catalyzed *cis*-cyclooctene oxidation [5,18]. This happens because proton abstraction from the allylic position of *cis*-cyclooctene generates a less stable radical than proton abstraction from the vinyllic position of this same substrate [18]. Indeed, the cyclooct-2-en-1-yl radical (allylic) can assume an unfavorable configuration, because *trans* interactions occur between the hydrogen atoms. To maintain the unsaturation and the radical structure in the same plane, the chain of the cyclooct-2-en-1-yl radical becomes distorted and, thus, less stable.

At a catalyst/oxidant/substrate molar ratio of 1:10:1000, MnP gave 54% *cis*-cyclooctene oxide yield compared with 4.5% achieved in the control reaction conducted in the absence of MnP (Table 2). Therefore, MnP really catalyzed *cis*-cyclooctene oxidation by PhIO. In the case of the heterogeneous system MnPS, the activity of the MnP was virtually maintained, but it decreased when MnPA and MnPB were used as catalysts.

In homogeneous medium, MnP afforded *cis*-cyclooctene oxide yield similar to those obtained with classic metalloporhyrins (MPs) such as metal(III) tetraphenylporphyrins, [M(TPP)] [81], the so-called first-generation porphyrins [3]. However, MnP provided lower product yield than those achieved with second-generation MPs (often between 80% and 100% epoxide yield). Second-generation MPs contain bulky groups (such as phenyl, alkoxy, and *tert*-butyl) or electron withdrawing substituents [3] at the *ortho* position of the *meso*-phenyl substituents in the porphyrin macrocycle [12]. These substituents activate the catalytic species, furnishing higher product yields than the first-generation MPs. The substituents in second-generation MPs also protect the catalyst against deactivation; more specifically, they avoid formation of non-catalytic species like dimeric species as well as catalyst self-destruction due to contact between the activated and the non-activated MP species [2–6]. We can consider the MnP studied in this paper as a first generation-like catalyst: its macrocyclic structure does not contain substituents that confer enough protection against deactivation effects, so the high-valence manganyl porphyrin (Mn(V)(O)Por), assumed as the catalytically active species [82] in this case, is less stable and gives product yields comparable to those attained with first-generation MPs [2–6].

MnPA and MnPB furnished lower product yield than homogeneous MnP. After immobilization, the catalytic species in MnPA and MnPB probably became less accessible to the reactants as compared with the MnP in solution [83].

MnPA, with six times lower MnP loading than MnPB, afforded larger product yield (35% and 27%, respectively, see Table 2). The textural properties of the silica-based MnPA and MnPB (Table 1) justify these results: MnPA has higher surface area and smaller pore size and volume. Hence, catalysis probably occurs on the surface of the MnPA catalyst, and not within its pores and interstices. UV–vis analysis of the supernatants of the reactions catalyzed by the silica-based catalysts did not detect any MnP, so the MP did not leach from either MnPA or MnPB.

The solid MnPS provided product yield higher than those obtained with the silica-based catalysts MnPA and MnPB and similar to that achieved with the MnP in homogeneous medium. Insoluble MnPS and MnP should have similar composition: MnPS should consist of MnP units structured in such a way that an insoluble solid exists in the reaction medium. The solid MnPS proved to be advantageous over the silica-based MnPA and MnPB for the following reasons: (i) whereas the MnP is diluted in the silica, due to the low catalyst loading in MnPA and MnPB, the surface of the solid MnPS consists of MnP. In other words, in MnPS the MnP is totally available to the approach of the substrate and the oxidant, so the reactants do not need to permeate into the structure of the solid to react with the active catalytic species. (ii) It is possible to recycle and reuse MnPS in more than one reaction, because MnPS is robust. To conduct the reuse reactions, we recovered MnPS from the reaction medium after the first use; we then washed, activated, and reused the recovered catalyst in a second reaction. Recycled MnPS gave virtually the same product yield as the fresh MnPS and the MnP in homogenous catalysis (Table 2). Indeed, FTIR analysis of MnPS after the first and second reaction confirmed its robustness: the recycled MnPS displayed the same spectral pattern as the freshly prepared MnPS (Fig. S3b, supplementary material). A catalytic test with manganese(II) acetate tetrahydrate – $Mn(OAc)_2{\cdot}4H_2O$ – was performed to evaluate the possible activity of Mn(II) centers. Epoxide of 17% yield was obtained (Table 2), showing that divalent Mn ion in solution can catalyze epoxidation and maybe, those present in MnPS can also have catalytic activity, since they are not blocked by metalloporphyrin ligands with their coordination spheres saturated, what does not allow reactants approximation.

MnPA and MnPB were also recycled for oxidation of cyclooctene and the yields obtained for epoxide formation were 31% (MnPA) and 23% (MnPB). These results show that manganese porphyrin immobilized onto silica still remains its catalytic activity.

We performed UV–vis analysis of the supernatant of each reaction that used the solid MnPS as catalyst. The reaction supernatant was colorless, indicating that the MnP did not leach from MnPS during catalysis. Therefore, this solid is robust and resistant to the catalytic conditions. Moreover, the absence of MnP in the supernatant of the reaction confirmed that the *cis*-cyclooctene oxidation by PhIO catalyzed by MnPS was a truly heterogeneous process. However, when we exposed MnPS to methanol, a small amount of the MnP solubilized in this solvent, and the solution acquired a green color. We calculated the loss of MnP in methanol and estimated it to be about 2%. Nevertheless, this mass loss did not interfere in the catalytic result because we conducted the *cis*-cyclooctene oxidation reaction in a different solvent.

Hydrogen peroxide, a green oxidant, was not investigated as oxidizing agent in this work because with manganese porphyrins it is necessary the use of a co-catalyst [21,84,85]. Also, for heterogeneous reactions, solids MnPS, MnPA and MnPB promote disproportionation of H_2O_2, not allowing its use.

3.3.2. Oxidation of cyclohexene

The oxidation of cyclohexene can take place at the vinyllic position, to give the epoxide, or at the allylic position, to produce the relative alcohol or ketone products. Therefore, cyclohexene oxidation poses a new challenge to researchers in the area of catalysis: scientists have sought to enhance its kinetics and promote different selectivity, once there is competition between the allylic and vinyllic routes [18–20,86,87]. In this paper, we investigated three different conditions regarding the amount of oxidant and substrate used during cyclohexene oxidation-conditions A, B, and C (see Table 3). All the studied MnP materials exhibited catalytic activity in the oxidation of cyclohexene by PhIO (Table 3).

In conditions A and B, MnP in homogeneous medium was selective toward the epoxide (Table 3, runs 1 and 2), as expected for catalysis using MPs [81]. In the absence of a catalyst, though, allylic oxidation is usually favored; indeed, the homogeneous reaction control (without MnP) conducted under condition B gave an epoxide/allylic product ratio equal to 0.21 (Table 3, run 16), while MnP afforded an epoxide/allylic product ratio equal to approximately 7.0, corroborating the selectivity of the latter catalyst toward the epoxide. It is noteworthy that conversion values (the amount of substrate converted in product) for catalyzed reactions in condition B are higher than those obtained from control reactions, proving that catalytic activity is due to metalloporphyrins molecules.

The oxidation of alkenes at the vinyllic position occurs via heterolytic transfer of the oxygen atom from the oxidant to the substrate. This route is favored in the case of PhIO, because this oxidant prevents the formation of radical species [19,20,56,88–92].

Condition C (Table 3, run 3), which employed a higher amount of substrate, significantly decreased the epoxide yield (44% to 31% from B to C, runs 2 and 3, respectively) and increased the formation of allylic products (from 6.6% to 44%, runs 2 and 3, respectively). This change in products ratio can be considered as a drop in the catalytic activity of MnP, because allylic products usually result from non-catalytic processes. Here, addition of larger volumes of cyclohexene makes the reaction solution more apolar, lowering the solubility of the MnP in the reaction medium. The reaction probably follows a non-catalytic pathway, which justifies the lower catalytic yields. In fact, the yields of allylic products obtained in run 3 were similar to those obtained in the control reaction (run 17).

Condition B gave the highest epoxide/allyllic products ratio for all the catalysts (homogeneous MnP and heterogeneous MnPS, MnPA, and MnPB) and also the highest conversion values, showing that this condition allowed for the best catalytic performance among the tested conditions and favored the vinyllic product.

In the case of heterogeneous catalysis (MnPS, MnPA, and MnPB), conditions A and C (Table 3, runs 4, 6, 9, 11, 12, and 14) afforded epoxide as well as a large amount of ketone. Despite exhaustive deaeration of the reaction vessels with argon purge, dioxygen still remained adsorbed onto the pores and surfaces of the catalysts. The presence of O_2 in the reaction medium favors formation of radical species, which quickly react with the substrate and generate the allylic radical, leading to the ketone [93]. By doubling the amount of PhIO (going from condition A to condition B), the epoxide yields increased for all the heterogeneous catalyst. Therefore, a greater amount of oxidant is necessary for the reaction to take place between the heterogenized MnP and the oxygen donor, leading to effective formation of the active catalytic species.

As observed in the case of *cis*-cyclooctene oxidation, MnPA furnished higher product yields than MnPB in all the conditions. Again, the textural properties of MnPA and MnPB justify these results: in MnPA, the MnP is located at the surface of the silica, facilitating the approach of PhIO and the substrate to the catalytic site, culminating in slightly better product yields. In the case of MnPB, its pores are ordered/cylindrical and open at both ends, facilitating

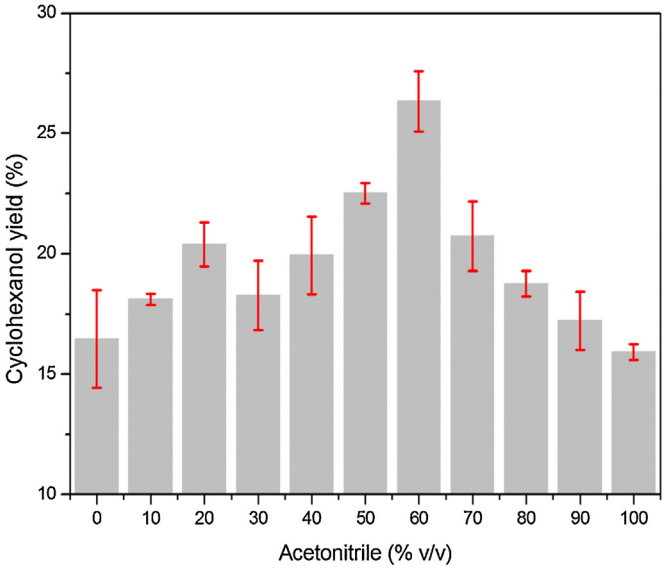

Fig. 5. Dependence of the cyclohexanol yield on the composition of the solvent mixture.

O_2 adsorption and favoring allylic products. In spite of the larger surface area of MnPA, O_2 adsorption onto this catalyst is more difficult: its pores are irregular and interconnected, which indicates the presence of ink-bottle pores, as discussed in the paragraph on nitrogen adsorption/desorption isotherms.

In condition B, the results attained with MnPS and homogeneous MnP were similar (Table 2, runs 5 and 2, respectively). As discussed for *cis*-cyclooctene oxidation, in MnPS the MnP is present as an organized structure, which favors the catalytic activity of this manganese(III) porphyrin.

We also investigated the main advantage of heterogeneous catalysts over homogeneous ones–catalyst reuse–in condition B, using MnPS (Table 3, runs 7 and 8). The recycled MnPS furnished total product yields similar to those obtained with the fresh MnPS under the same condition (Table 3, run 5), with high selectivity for the epoxide. Hence, MnPS is a robust and reusable solid catalyst.

3.3.3. Oxidation of cyclohexane

The inert nature of saturated C–H bonds and the different chemo- and regioselectivities achieved during alkane oxidation using different oxidants and catalysts makes alkane functionalization a challenging task [12,94]. In this study, we employed cyclohexane, to probe the chemoselectivity (formation of cyclohexanol, c-ol, and/or cyclohexanone, c-one) and *n*-heptane, to monitor both the chemo (production of heptanol or heptanone) and regioselectivity (oxidation at different positions of the carbon chain) of the prepared catalysts. We did not investigate diols, aldehydes, carboxylic acids, or other *n*-heptane oxidation products.

Concerning the oxidation of cyclohexane, all the studied catalysts were selective for the alcohol (Table 4, runs 1 to 4), with c-ol/c-one ratios ranging from 5 to 16. The control reactions did not yield any product (Table 4, runs 5 and 6), showing that it is difficult to oxidize cyclohexane in the absence of a catalyst.

As expected for metalloporphyrin-catalyzed cyclohexane oxidation, the homogeneous catalyst MnP (run 1) was selective toward the alcohol [93]. Indeed, this MnP provided greater yields than first-generation MPs ([Fe(TPP), 8% yield for cyclohexanol, in DCM [20,31,95,96]; [Mn(TAPP)], 27% yield cyclohexanol [3,50]).

In an attempt to achieve better performance in the catalytic oxidation of cyclohexane in homogeneous medium, we studied how the DCM/ACN volume ratio affected the process (Fig. 5). We found that the pure solvents (ACN or DCM) led to the worst results.

Table 3
Yields of oxidation products from cyclohexene oxidation by PhIO catalyzed by MnP systems[a].

Catalyst	Run	Condition[b]	Product yields (%)[c]			Ratio[d]	Conversion (10^{-3})[e]
			Oxide	Alcohol	Ketone		
MnP[f]	1	A	39	6.1	19	1.56	5.46
	2	B	44	3.0	3.3	6.98	9.73
	3	C	31	5.4	39	0.70	2.23
MnPS	4	A	24	4.5	26	0.77	4.15
	5	B	46	3.0	7.0	4.6	10.5
	6	C	24	8.1	48	0.43	2.24
1st reuse	7	B	38	3.2	4.6	4.87	8.70
2nd reuse	8	B	36	2.6	5.9	4.23	8.31
MnPA	9	A	12	6.0	37	0.27	3.65
	10	B	17	4.2	8.8	1.3	5.12
	11	C	21	10	42	0.40	2.08
MnPB	12	A	8.5	5.0	30	0.24	2.85
	13	B	14	1.7	3.6	2.6	3.50
	14	C	20	5.0	21	0.77	1.42
PhIO[g]	15	A	8.1	9.0	66	0.11	5.01
	16	B	8.9	3.0	40	0.21	6.38
	17	C	14	7.4	48	0.25	1.81
Silica + PhIO[h]	18	A	12	8.5	55	0.19	4.80
	19	B	10	5.5	26	0.32	5.70
	20	C	17	8.0	32	0.42	1.64

[a] Reactions carried out in duplicate. Reaction conditions: argon atmosphere, absence of light, magnetic stirring, room temperature, 60 min, DCM/ACN 1:1 (v/v) solvent mixture. [b]Conditions relate to the different catalyst/PhIO/cyclohexene molar ratios used in the experiments: A—1:10:1000; B—1:20:1000; C—1:20:5000.
[c] Yields based on PhIO-oxide = cyclohexenoxide, alcohol = cyclohexen-1-ol, ketone = cyclohexen-1-one.
[d] Ratio between epoxide yield and the sum of alcohol and ketone yields.
[e] Conversion is defined by the total amount of substrate that is converted in products and is dimensionless. For conversion values determination, it was considered that 2 mols of PhIO are necessary to form 1 mol of ketone.
[f] Homogeneous catalysis.
[g] Homogeneous control reaction.
[h] Heterogeneous control reaction.

Table 4
Yields of oxidation products from alkane oxidation by PhIO catalyzed by MnP systems[a].

Catalyst	Run	Cyclohexane oxidation product yield (%)[b]			Run	*n*-Heptane oxidation product yield (%)[c]		
		c-ol	c-one	Ratio c-ol/c-one		c-ol (total)	c-one (total)	TSI index
MnP[d]	1	21	1.3	16	7	13	1.1	53.5
MnPS	2	12	1.3	9.2	8	3.4	1.1	59.4
MnPA	3	6.3	1.2	5.2	9	2.6	1.2	53.8
MnPB	4	5.0	0.7	7.1	10	2.1	1.0	52.3
PhIO[e]	5	–	–	–	11	–	–	–
Silica[f]	6	–	–	–	12	–	–	–

[a] Reactions carried out in duplicate. Reaction conditions: argon atmosphere, absence of light, magnetic stirring, room temperature, 60 min, DCM/ACN 1:1 (v/v) solvent mixture.
[b] Yields based on PhIO–c-ol = cyclohexanol and c-one = cyclohexanone.
[c] Yields based on PhIO–c-ol (total) = total heptanol yields percentage resulted from the alcohol at carbon position 1, 2, 3, of the linear alkane and c-one (total) = total heptanone yields percentage resulted from the alcohol at carbon position 2 and 3, of the linear alkane. TS index = terminal selectivity index.
[d] Homogeneous catalysis.
[e] Homogeneous control reaction.
[f] Heterogeneous control reaction.

Because the MnP is more soluble in ACN, we had expected that increased ACN content in the solvent mixture would favor the catalytic activity. However, the substrate and PhIO are poorly soluble in ACN, which accounts for the lower product yields. As for DCM, the substrate cyclohexane is highly soluble in this solvent, whereas the MnP and PhIO have low solubility in this same solvent. In the end, DCM/ACN 4:6 v/v was the solvent mixture that afforded the best cyclohexanol yields, 26%, which is five percentage points above the standard conditions used in this study (Table 4, DCM/ACN 1:1 v/v, run 1) [97]. We did not detect any significant formation of ketone in most of the solvent proportions used here (values below 1.4%).

As expected, the heterogeneous catalysts MnPS, MnPA, and MnPB led to lower product yields than homogeneous MnP. Two factors operate in the case of MnPA and MnPB: the difficult interaction between the MnP diluted in the solid matrix (Table 4, runs 3 and 4) and the inertia of cyclohexane when compared with unsaturated substrates [2]. Again, MnPS (run 2) was the best heterogeneous catalyst for substrate oxidation, for the same reasons already discussed in items 3.3.1 and 3.3.2—the high catalyst density per mass of solid catalyst as compared with the silica-based solids MnPA and MnPB.

3.3.4. Oxidation of n-heptane

The structure of *n*-heptane, the most inert substrate investigated in this paper, contains five secondary carbons, which are more labile to oxidation, and two primary carbons (carbons at position 1 and 7), which are more inert to the oxidation reaction due to thermodynamic factors and the low stability of the radical formed at these positions [94]. Both thermodynamics and statistics are expected to influence the distribution of the products. Yields of 3- and 2-heptanol should be similar; the yield of 4-heptanol should be half the yield achieved for 3- and 2-heptanol. There should not be significant formation of 1-heptanol, because of the higher inertia of the C–H bonds of the primary carbons at positions 1 and 7 of *n*-heptane [53].

As in the case of cyclohexane, all the catalysts used here were selective for alcohol (Table 4, runs 7 to 10), mainly MnP in homogenous system (run 7). The catalytic yields obtained with *n*-heptane were low, confirming that this linear alkane is inert to oxidation [2]. The homogeneous and heterogeneous control reactions (runs 11 and 12, respectively) did not afford any products, as expected for the oxidation of a highly inert substrate.

Interestingly, all the catalysts based on the MnP used in this work were more selective for 1- and 2-heptanol, and not for 2- and 3-heptanol, as expected if one considers the statistical and thermodynamic factors [94]. To better illustrate this selectivity, we introduced an index that correlates the linear alkane oxidation at carbons 1 and 2, the terminal selectivity index (TSI), defined as the ratio between the sums of the yields of 1- and 2-heptanol and the total alcohol yield obtained in the oxidation of *n*-heptane. This index is similar to the primary selectivity index set by Cook et al. [98]; the difference is that the latter authors only considered oxidation at the primary carbon, whilst TSI takes into account both highly hindered and less hindered positions (Table 4). Heterogeneous catalytic systems promote the terminal oxidation of linear hydrocarbons when (i) the structure of the catalyst is able to stabilize the less thermodynamically favored intermediate and (ii) the geometry of the solid catalyst only allows for the approach of the terminal carbon of the substrate to the active catalytic species. Thomas et al. [53] described that aluminophosphate molecular sieves (AlPOs) doped with transition metals and bearing pores and channels can catalyze the oxidation of alkanes in air. The latter system was highly selective for the terminal carbon of alkanes, because the channels in the solid allowed the substrate to arrive at the catalytic species in an end-on approach.

Porphyrin systems in homogeneous medium can also promote the oxidation of alkanes at terminal positions. Cook et al. [98] reported that the manganese(III) porphyrin [Mn(TTPPP)] was selective toward the primary alcohol when it was used as catalyst for hexane oxidation in a homogenous system. In this case, the authors attributed the selectivity for the primary carbon to steric factors within the porphyrin itself, and not to a cage formed by a solid matrix. The 2,4,6-triphenyl phenyl substituent at the *meso* positions of [Mn(TTPPP)] hindered the approach of the substrate by creating a structure similar to the cavities found in solid supports. As a result, only the terminal carbon of the linear alkane was able to approach the metal center, to give 1-hexanol.

Using [Mn(TTMPP)] as catalyst, a porphyrin containing three methoxy groups instead of the three phenyl substituents in [Mn(TTPPP)], Nappa and Tollman [99] showed catalytic selectivity for the carbon at position 2 of hexane, because the substituents in [Mn(TTMPP)] were not as bulky as the substituents in [Mn(TTPPP)]. Therefore, thermodynamic factors operated in this case: because carbon 2 was accessible, it was oxidized rather than the primary carbon. We applied TSI for [Mn(TTMPP)] and found a value of 52.0% against the 53.5% reached for MnP. Hence, extremely bulky groups like the ones in Mn(TTPPP) or moderately bulky substituents like the ones in Mn(TTMPP) are not necessary to achieve oxidation at positions 1 or 2.

A TSI around 40% was expected for a thermodinamically corrected statistical distribution of the products (contribution of 40% from C2 and none from C1). We obtained TSI values higher than 40% for all the investigated catalysts, a value that was also reported for [Mn(TTMPP)], a recognized manganese(III) porphyrin for the selective oxidation of heptane. MnP has methoxy groups only at one *meta* position of its phenyl rings, thereby posing lower steric hindrance to the approach of the substrate as compared with [Mn(TTMPP)]. In the case of porphyrins that can form *atropisomers*, the statistical distribution that leads to the most stabilized spatial configuration is the one that presents three of the four phenyl rings pointing upward and one phenyl ring facing downward relative to the plane of the porphyrin ring. In the case of the MnP, this configuration restricts the approach of the substrate to the metal center, explaining the higher TSI values [99,100].

4. Conclusion

In an attempt to solve problems related to homogeneous catalysis mediated by metalloporphyrins, several strategies were developed by various groups in the last three decades, such as addition of electron-withdrawing groups at the *meso*-phenyl substituints, and heterogenization onto different inert matrices or by self-assembly methodologies. Diverting chemical functionalization options, that would modify the intrinsic characteristic of the hydroxyl–methoxyphenyl substituted porphyrin applied in this work, heterogenization techniques were developed with success. Immobilization of the manganeseporphyrin onto silica by the sol–gel process afforded materials with different compositional, textural and morphological characteristics and reactivities towards oxidation of different hydrocarbons.

Self-assembly of manganese(III) porphyrins and Mn(II) centers resulted in an insoluble interesting solid, that showed catalytic activities similar to those obtained in homogeneous systems and high selectivity for epoxidation of alkenes and hydroxylation of alkanes. This material has the advantage of being recyclable and robust, what goes with characteristic of desired new materials, such as coordination polymers and metal-organic frameworks.

Acknowledgments

The authors acknowledge the financial support obtained from CAPES (Coordenação de Aperfeiçoamento de Pessoal de Nivel Superior), CNPq (Conselho Nacional de Desenvolvimento Científico e Tecnológico), FINEP (Financiadora de Estudos e Projetos), and Araucária Foundation. We are also thankful for the technical support of FUNPAR (Fundação da Universidade Federal do Paraná) and UFPR (Universidade Federal do Paraná).

Appendix A. Supplementary data

Supplementary data associated with this article can be found, in the online version, at http://dx.doi.org/10.1016/j.molcata.2013.06.022.

References

[1] B. Meunier, Bull. Soc. Chim. Fr. 4 (1986) 578–594.
[2] D. Mansuy, Pure Appl. Chem. 62 (1990) 741–746.
[3] D. Dolphin, T.G. Traylor, L.Y. Xie, Acc. Chem. Res. 30 (1997) 251–259.
[4] F. Bedioui, Coord. Chem. Rev. 144 (1995) 39–68.
[5] D.R. Leanord, J.R. Lindsay-Smith, J. Chem. Soc., Perkin Trans. 2 1 (1991) 25–30.
[6] B. Meunier, Chem. Rev. 92 (1992) 1411–1456.
[7] E.D. Sternberg, D. Dolphin, Tetrahedron 54 (1998) 4151–4202.
[8] M. Ethirajan, Y. Chen, P. Joshi, R.K. Pandey, Chem. Soc. Rev. 40 (2011) 340–362.
[9] M. Biesaga, K. Pyrzyn'ska, M. Trojanowicz, Talanta 51 (2000) 209–224.
[10] I. Beletskaya, V.S. Tyurin, A.Y. Tsivadze, R. Guilard, C. Stern, Chem. Rev. 109 (2009) 1659–1713.
[11] M.G. Walter, A.B. Rudine, C.C. Wamser, J. Porphyrins Phthalocyanines 14 (2010) 759–792.
[12] M. Costas, Coord. Chem. Rev. 255 (2011) 2912–2932.
[13] F. Wypych, G.A. Bubniak, M. Halma, S. Nakagaki, J. Colloid Interface Sci. 264 (2003) 203–207.
[14] K.S. Suslick, P. Bhyrappa, J.H. Chou, M.E. Kosal, S. Nakagaki, D.W. Smithenry, S.R. Wilson, Acc. Chem. Res. 38 (2005) 283–291.
[15] J.Y. Lee, O.K. Farha, J. Roberts, K.A. Scheidt, S.B.T. Nguyen, J.T. Hupp, Chem. Soc. Rev. 38 (2009) 1450–1459.
[16] O.K. Farha, J.T. Hupp, Acc. Chem. Res. 43 (2010) 1166–1175.
[17] G.S. Machado, G.C.G. Arizaga, F. Wypych, S. Nakagaki, J. Catal. 274 (2010) 130–141.
[18] A.J. Appleton, S. Evans, J.R. Lindsay-Smith, J. Chem. Soc., Perkin Trans. 2 (1995) 281–285.
[19] J.R. Lindsay-Smith, P.R. Sleath, J. Chem. Soc., Perkin Trans. 2 (1982) 1009–1015.
[20] J.T. Groves, T.E. Nemo, J. Am. Chem. Soc. 105 (1983) 6243–6248.

[21] P.C. Cooke, J.R. Lindsay-Smith, J. Chem. Soc., Perkin Trans. 1 (1994) 1913–1923.
[22] F. Doro, J.R. Lindsay Smith, A.G. Ferreira, M.D. Assis, J. Mol. Catal. A: Chem. 164 (2000) 97–108.
[23] A.A. Guedes, J.R. Lindsay Smith, O.R. Nascimento, D.F.C. Guedes, M.D. Assis, J. Braz. Chem. Soc. 16 (2005) 835–843.
[24] S. Evans, J.R. Lindsay Smith, J. Chem. Soc., Perkin Trans. 2 (2001) 174–180.
[25] O. Leal, D.L. Anderson, R.G. Bowman, F. Basolo, R.L. Burwell Jr., J. Am. Chem. Soc. 97 (1975) 5125–5129.
[26] P. Battioni, J.-P. Lallier, L. Barloy, D. Mansuy, J. Chem. Soc., Chem. Commun. (1989) 1149–1151.
[27] P. Battioni, J.F. Bartoli, D. Mansuy, Y.S. Byun, T.G. Traylor, J. Chem. Soc., Chem. Commun. (1992) 1052–1053.
[28] D. Mansuy, Coord. Chem. Rev. 125 (1993) 129–141.
[29] S. Nakagaki, G.K.B. Ferreira, G.M. Ucoski, K.A.D.F. Castro, Molecules 18 (2013) 7279–7308.
[30] T. Matsui, M. Iwasaki, R. Sugiyama, M. Unno, M. Ikeda-Saito, Inorg. Chem. 49 (2010) 3602–3609.
[31] S. Nakagaki, A.R. Ramos, F.L. Benedito, P.G. Peralta-Zamora, A.J.G. Zarbin, J. Mol. Catal. A: Chem. 185 (2002) 203–210.
[32] A.M. Machado, F. Wypych, S.M. Drechsel, S. Nakagaki, J. Colloid Interface Sci. 254 (2002) 158–164.
[33] M. Halma, F. Wypych, S.M. Drechsel, S. Nakagaki, J. Porphyrins Phthalocyanines 6 (2002) 502–513.
[34] S. Nakagaki, M. Halma, A. Bail, G.G.C. Arízaga, F. Wypych, J. Colloid Interface Sci. 281 (2004) 417–423.
[35] G.S. Machado, F. Wypych, S. Nakagaki, Appl. Catal., A 413–414 (2012) 94–102.
[36] S. Nakagaki, K.A.D.F. Castro, G.S. Machado, M. Halma, S.M. Drechsel, F. Wypych, J. Braz. Chem. Soc. 17 (2006) 1672–1678.
[37] S. Nakagaki, A.S. Mangrich, F. Wypych, Inorg. Chim. Acta 254 (1997) 213–217.
[38] A.T. Papacıdero, L.A. Rocha, B.L. Caetano, E. Molina, H.C. Sacco, E.J. Nassar, Y. Martinelli, C. Mello, S. Nakagaki, K.J. Ciuffi, Colloids Surf., A 275 (2006) 27–35.
[39] A.M. Shultz, O.K. Farha, J.T. Hupp, S.B.T. Nguyen, J. Am. Chem. Soc. 131 (2009) 4204–4205.
[40] A. Dhakshinamoorthy, M. Alvaro, Y.K. Hwang, Y.K. Seo, A. Corma, H. Garcia, Dalton Trans. 40 (2011) 10719–10724.
[41] D.J. Tranchemontagne, J.L. Mendoza-Cortes, M. O'Keeffe, O.M. Yaghi, Chem. Soc. Rev. 38 (2009) 1257–1283.
[42] S. Motoyama, R. Makiura, O. Sakata, H. Kitagawa, J. Am. Chem. Soc. 133 (2011) 5640–5643.
[43] P. Bhyrappa, K.S. Suslick, J. Am. Chem. Soc. 119 (1997) 8492–8502.
[44] M.E. Kosal, K.S. Suslick, J. Solid State Chem. 152 (2000) 87–98.
[45] J. Chou, M.E. Kosal, H.S. Nalwa, N.A. Rakow, K.S. Suslick, The Porphyrin Handbook, Academic Press, New York, 2000.
[46] D.W. Smithenhy, S.R. Wilson, K.S. Suslick, Inorg. Chem. 42 (2003) 7719–7721.
[47] W. Stöber, A. Fink, E. Bohn, J. Colloid Interface Sci. 26 (1998) 62–69.
[48] X. Liang, J. Xiao, B. Chen, Y. Li, Inorg. Chem. 49 (2010) 8188–8190.
[49] K.A.D.F. Castro, M. Halma, G.S. Machado, G.P. Ricci, G.M. Ucoski, K.J. Ciuffi, S. Nakagaki, J. Braz. Chem. Soc. 21 (2010) 1329–1340.
[50] G.M. Ucoski, K.A.D.F. Castro, K.J. Ciuffi, G.P. Ricci, J.A. Marques, F.S. Nunes, Appl. Catal., A 404 (2011) 120–128.
[51] S. Farhadi, Saeid, A. Zabardasti, M.H. Rahmati, J.Chem. Res. 3 (2011) 157–160.
[52] J.H. Cai, J.W. Huang, P. Zhao, Y.J. Ye, H.C. Yu, L.N. Ji, J. Sol–Gel Sci. Technol. 50 (2009) 430–436.
[53] M.J. Thomas, R. Raja, G. Sankar, R.G. Bell, Acc. Chem. Res. 34 (2001) 191–200.
[54] A.D. Adler, F.R. Longo, J.D. Finarelli, J. Goldmacher, J. Assour, L. Koakoff, J. Org. Synth. 32 (1967) 476.
[55] J.L. Nian, L. Min, H.A. Kong, Inorg. Chim. Acta 178 (1990) 59–65.
[56] E. Baciocchi, F. d'Acunzo, C. Galli, M. Loele, J. Chem. Soc., Chem. Commun. (1995) 429–430.
[57] H. Saltzman, J.G. Sharefkin, Org. Synth. 5 (1963) 60–61.
[58] H. Kobayashi, T. Higuchi, Y. Kaizu, H. Osada, M. Aoki, Bull. Chem. Soc. Jpn. 48 (1975) 3137–3141.
[59] W. Zheng, N. Shan, L. Yu, X. Wang, Dyes Pigm. 77 (2008) 153–157.
[60] J.B. Allison, R.S. Becker, J. Chem. Phys. 32 (1960) 1410–1417.
[61] L.J. Boucher, J. Am. Chem. Soc. 92 (1970) 2725–2730.
[62] M.T. Caudle, C.K. Mobley, L.M. Bafaro, R. Lobrutto, G.T. Yee, T.L. Groy, Inorg. Chem. 43 (2004) 506–514.
[63] K. Nakamoto, Infrared and Raman Spectra of Inorganic and Coordination Compounds parts A and B, fifth ed., Wiley Interscience Publication, Hoboken, NJ, 2000.
[64] G.B. Deacon, R.J. Phillips, Coord. Chem. Rev. 33 (1980) 227–250.
[65] E-Y. Choi, P.M. Barron, R.W. Novotny, H-T. Son, C. Hu, W. Choe, Inorg. Chem. 48 (2009) 426–428.
[66] A.M. Shultz, O.K. Farha, J.T. Hupp, S.T. Nguyen, J. Am. Chem. Soc. 131 (2009) 4204–4205.
[67] S. Roy, C.B. George, M.A. Ratner, J. Chem. Phys. C 116 (2012) 23494–23502.
[68] K.A. Campbell, M.R. Lashley, J.K. Wyatt, M.H. Nantz, R.D. Britt, J. Am. Chem. Soc. 123 (2001) 5710–5719.
[69] M.A. Vázquez-Fernández, M.R. Bermejo, M.I. Fernández-García, G. González-Riopedre, M.J. Rodríguez-Doutón, M. Maneiro, J. Inorg. Biochem. 105 (2011) 1538–1547.
[70] M. Halma, K.A.D.F. Castro, V. Prévot, C. Forano, F. Wypych, S. Nakagaki, J. Mol. Catal. A: Chem. 310 (2009) 42–50.
[71] R. Makiura, S. Motoyama, Y. Umemura, H. Yamanaka, O. Sakata, H. Kitagawa, Nat. Mater. 9 (2010) 565–571.
[72] T. Ohmura, A. Usuki, K. Fukumori, T. Ohta, M. Ito, K. Tatsumi, Inorg. Chem. 45 (2006) 7988–7990.
[73] D.W. Smithenry, S.R. Wilson, K.S. Suslick, Inorg. Chem. 42 (2003) 7719–7721.
[74] G.R. Friedermann, A.S. Mangrich, M. Halma, K.A.D.F. Castro, F.L. Benedito, F.G. Doro, S.M. Drechsel, M.D. Assis, S. Nakagaki, Appl. Catal., A 308 (2006) 172–181.
[75] C.J. Brinker, G.W. Scherer, Sol–Gel Science: The Physics and Chemistry of Sol–Gel Processing, first ed., Academic Press, San Diego, 1990.
[76] A.M. Buckley, M. Greenblatt, J. Chem. Edu. 71 (1994) 599–602.
[77] L.L. Hench, J.K. West, Chem. Rev. 90 (1990) 33–72.
[78] G.S. Machado, K.A.D.F. Castro, O.J. Lima, E.J. Nassar, K.J. Ciuffi, S. Nakagaki, Colloids Surf., A 349 (2009) 162–169.
[79] K.S.W. Sing, D.H. Everett, R.A.W. Haul, L. Moscou, R.A. Pierotti, J. Rouquerol, T. Siemieniewska, Pure Appl. Chem. 57 (1985) 603–619.
[80] A. Grosman, C. Ortega, Langmuir 21 (2005) 10515–10521.
[81] J.T. Groves, T.E. Nemo, R.S. Myers, J. Am. Chem. Soc. 101 (1979) 1032–1033.
[82] J.T. Groves, W.J. Kruper, R.C. Haushalter, J. Am. Chem. Soc. 102 (1980) 6375–6377.
[83] S. Nakagaki, G.S. Machado, M. Halma, A.A.S. Marangon, K.A.D.F. Castro, N. Mattoso, F. Wypych, J. Catal. 242 (2006) 110–117.
[84] T. Tatsumi, M. Nakamura, H. Tominaga, Catal. Today 6 (1989) 163–170.
[85] M. Moghadam, V. Mirkhani, S. Tangestaninejad, I. Mohammdpoor-Baltork, H. Kargar, J. Mol. Catal. A: Chem. 288 (2008) 116–124.
[86] J.T. Groves, D.V. Adhyam, J. Am. Chem. Soc. 106 (1984) 2177–2181.
[87] E.C. Zampronio, M.C.A.F. Gotardo, M.D. Assis, H.P. Oliveira, Catal. Lett. 104 (2005) 53–56.
[88] T. Oyama, Mechanisms in Homogeneous and Heterogeneous Epoxidation Catalysis, first ed., Elsevier, Amsterdam, 2008.
[89] J.T. Groves, D.V. Subramanian, J. Am. Chem. Soc. 106 (1984) 2177–2181.
[90] J.T. Groves, M.K. Stern, J. Am. Chem. Soc. 110 (1980) 8628–8633.
[91] T.G. Traylor, A.R. Miksztal, J. Am. Chem. Soc. 111 (1989) 7443–7448.
[92] M.J. Nappa, R.J. McKinney, Inorg. Chem. 27 (1988) 3740–3745.
[93] J.R. Lindsay-Smith, Y. Iamamoto, F.S. Vinhado, J. Mol. Catal. A: Chem. 252 (2006) 23–30.
[94] J.M. Thomas, J.C. Hernandez-Garrido, R. Raja, R.G. Bell, Phys. Chem. Chem. Phys. 11 (2009) 2799–2825.
[95] S. Nakagaki, C.R. Xavier, A.J. Wosniak, A.S. Mangrich, F. Wypych, M.P. Cantão, I. Denicoló, L.T. Kubota, Colloids Surf., A 168 (2000) 261–276.
[96] Y. Iamamoto, Y.M. Idemori, S. Nakagaki, J. Mol. Catal. A: Chem. 99 (1995) 187–193.
[97] Y. Iamamoto, M.D. Assis, K.J. Ciuffi, H.C. Sacco, L. Iwamoto, A.J.B. Melo, O.R. Nascimento, C.M.C. Prado, J. Mol. Catal. A: Chem. 109 (1996) 189–200.
[98] B.R. Cook, T.J. Reinert, K.S. Suslick, J. Am. Chem. Soc. 108 (1986) 7281–7286.
[99] M.J. Nappa, C.A. Tolman, Inorg. Chem. 24 (1985) 4711–4719.
[100] L.K. Gottwald, E.F. Ullman, Tetrahedron Lett. 36 (1969) 3071–3074.